Nuclear Fluxes in Diatomic Molecules Deduced from Pump-Probe Spectra with Spatiotemporal Resolutions down to 5 pm and 200 asec

Jörn Manz*

State Key Laboratory of Quantum Optics and Quantum Optics Devices, Institute of Laser Spectroscopy, Shanxi University, 92 Wucheng Road, Taiyuan 030006, China and Institut für Chemie und Biochemie, Freie Universität Berlin, Takustraße 3, 14195 Berlin, Germany

Jhon Fredy Pérez-Torres

Institut für Chemie und Biochemie, Freie Universität Berlin, Takustraße 3, 14195 Berlin, Germany

Yonggang Yang

State Key Laboratory of Quantum Optics and Quantum Optics Devices, Institute of Laser Spectroscopy, Shanxi University, 92 Wucheng Road, Taiyuan 030006, China

(Received 1 June 2013; published 10 October 2013)

When molecules move, their nuclei flow. The corresponding quantum observable, i.e., the nuclear flux density, was introduced by Schrödinger in 1926, but until now, it has not been measured. Here the first experimental results are deduced from high-resolution pump-probe measurements of the time-dependent nuclear densities in a vibrating diatomic molecule or molecular ion. The nuclear densities are converted to flux densities by means of the continuity equation. The flux densities are much more sensitive to time-dependent quantum effects than the densities. Applications to the sodium molecule and the deuterium molecular ion unravel four new effects; e.g., at the turns from bond stretch to compression, the flux of the nuclei exhibits multiple changes of directions, from small to large bond lengths, a phenomenon that we call the ''quantum accordion.''

DOI: 10.1103/PhysRevLett.111.153004 PACS numbers: 33.20.Xx, 82.53.−k, 82.53.Hn

Panta rhei—everything flows. Today, this famous hypothesis [1] has been confirmed in almost all fields of physics. Prominent examples in molecular physics, atomic physics, attosecond and strong field physics, and neighboring fields, e.g., physical chemistry, femtosecond chemistry, and molecular engineering include fluxes of molecules in molecular beams [2,3] or of electrons through molecules between electrodes [4,5], or laser-induced electron tunneling current flow in atoms [6]. Until now, however, intramolecular nuclear fluxes have not been monitored experimentally. The first purpose of this Letter is to open experimental access to this demanding field, specifically to nuclear fluxes in diatomic molecules. It calls for a new record in spatiotemporal resolution of experimental flux densities $\tilde{j}_R(R, t)$, which depend on internuclear bond distance (R) and time (t) [i.e., better than 10 picometers (pm) and from ~20 femtoseconds (fs) down to 200 attoseconds (asec), respectively]. For comparison, this standard has already been achieved in recent quantum dynamics simulations of wave packet interferometry for nuclear densities and flux densities in the vibrating iodine molecule I_2 [7]. The flux density $\tilde{j}_R(R, t)$ is related to the time-dependent density $\tilde{\rho}(R, t)$ by means of the continuity equation [8]; see Eqs. (1) and (2) together with the definitions given below. There is, in principle, no way in which to measure $\tilde{j}_R(R, t)$ independently of $\tilde{\rho}(R, t)$, simultaneously, since that would violate the uncertainty principle. The first goal of this Letter is understood in this context. The second purpose is to use the nuclear flux densities to reveal new, possibly even counterintuitive, quantum effects. For reference, it is intuitively clear that a vibrating diatomic molecule exhibits alternating stretches and compressions of the chemical bond. Accordingly, in a classical picture, the velocity $v_{cl} = \dot{R}$ and hence the nuclear flux density $j_{cl} = \rho_{cl} v_{cl}$ (where ρ_{cl} denotes the classical nuclear density) should oscillate between positive and negative values, respectively. As a working hypothesis, one could assume that the experimental nuclear flux density $\tilde{j}_R(R, t)$ should evolve analogously. Since the experimental results account inherently for the underlying quantum dynamics, any deviations from the classical reference should reveal new quantum phenomena.

This Letter presents the first experimental nuclear flux densities $\tilde{j}_R(R, t)$ of vibrating diatomic molecules or molecular ions, specifically for the Na_2 molecule in the electronic excited state $2^1\Pi_g$, and for the D_2^+ molecular ion in the electronic ground state $^2\Sigma_g^+$. Our choice of these systems is motivated by two criteria. First, the original experimental papers by Frohnmeyer and Baumert for $Na_2(2^1\Pi_g)$ [9] as well as by Ullrich, Moshammer, and co-workers for $D_2^+(^2\Sigma_g^+)$ [10] not only present the original pump-probe spectra, but they also convert them to nuclear probability densities $\tilde{\rho}(R, t)$. The signals for $\tilde{\rho}(R, t)$ are integrated over all molecular orientations (Θ, Φ), i.e., $\tilde{\rho}(R, t) \equiv \rho(R, t)R^2 = \int d\Omega |\psi(R, \Theta, \Phi, t)|^2$ for the corresponding

molecular wave function $\Psi(R, \Theta, \Phi, t) = \psi(R, \Theta, \Phi, t)/R$, in accord with quantum dynamics simulations of $\tilde{\rho}(R, t)$ in Refs. [11,12], respectively. The experimental $\tilde{\rho}(R, t)$ provide an important intermediate step from the original pump-probe spectra to the corresponding target observable $\tilde{j}_R(R, t) \equiv j_R(R, t)R^2$. Since $\tilde{\rho}(R, t)$ evolves ultrafast in one dimension, we use the unit 1/fs (1 fs = 10^{-15} s) of $\tilde{j}_R(R, t)$, which is the same as the unit used for the nuclear flux at R and t. The pump-probe measurement of the nuclear flux density in a vibrating diatomic molecule is, therefore, equivalent to monitoring the nuclear flux. Second, the spatiotemporal resolutions of the densities are 17 fs and 4 pm for $Na_2(2^1\Pi_g)$, and 220 asec and 5 pm for $D_2^+(^2\Sigma_g^+)$, respectively. These extraordinarily high resolutions are essential for the present purpose. They were achieved by means of femtosecond photoelectron spectroscopy [9,13] (based on theoretical concepts and simulations of Refs. [11,14]), or by time-resolved three-dimensional Coulomb explosion imaging [10] (based on concepts of Ref. [15]). We are not aware of any other published pump-probe spectra of vibrating diatomic molecules with similar high resolutions; very recently, S. R. Leone presented analogous results for the Br_2 molecule [16]. For comparison, these methodological advances [9,10] improve the spatiotemporal resolutions of the pioneering femtosecond pump-probe experiments of Zewail [17,18] by approximately one order of magnitude.

The experimental nuclear densities $\tilde{\rho}(R, t)$ are shown in Figs. 1(a) and 2(a) for vibrating $Na_2(2^1\Pi_g)$ and $D_2^+(^2\Sigma_g^+)$, adapted from Refs. [9,10], respectively. Their spatiotemporal patterns appear as mountains with oscillatory ridges. These correspond to quasiperiodic alternating bond stretches and compressions. Four vibrational periods are displayed in the time windows for Figs. 1 and 2. These are chosen such that the pump and probe laser pulses do not overlap (their full widths at half maximum are 40 fs for Na_2 and 7 fs for D_2^+). Another reason for the choice of these time windows is that they correspond to entirely different mechanisms of the vibrational dynamics. The point that we wish to make here is that the method to obtain $\tilde{j}_R(R, t)$ from $\tilde{\rho}(R, t)$ deduced from pump-probe spectra is general. To distinguish these mechanisms, we recall that in pump-probe spectroscopy of diatomic molecules, the pump laser pulse induces quasiperiodic sequences of three phases of the vibrational quantum dynamics: (i) vibrational round trips that correspond to classical motion, (ii) quantum dispersion of the wave packet, and (iii) vibrational revivals [19]. The time windows for Figs. 1 and 2 show $Na_2(2^1\Pi_g)$ in phase (i) and $D_2^+(^2\Sigma_g^+)$ in phase (ii). Figure 1(a) displays rather large amplitude (internuclear distances between ~3.0 to 5.0 Å) vibrations for $Na_2(2^1\Pi_g)$, with typical round-trip times of about 370 fs. In contrast, the overall shape of the nuclear density for $D_2^+(^2\Sigma_g^+)$ shown in Fig. 2(a) is quite robust [see also Fig. 4(a) below]. It appears as rather a broad "mountain" ranging from ~1.0 to 3.5 Å. The top of this mountain shakes with rather small amplitude (say from 1.7 to 2.1 Å) and short period ($\tau = 3$ fs), which correlates well with the period of the pump laser pulse. This is a consequence of its very high intensity ($I_{max} \approx 0.5 \times 10^{15}$ W/cm^2) for $D_2^+(^2\Sigma_g^+)$, which causes field dressing of the molecular ion, shaking it at the frequency of the pump pulse [10,20]. This effect does not occur in the photoelectron spectroscopy of

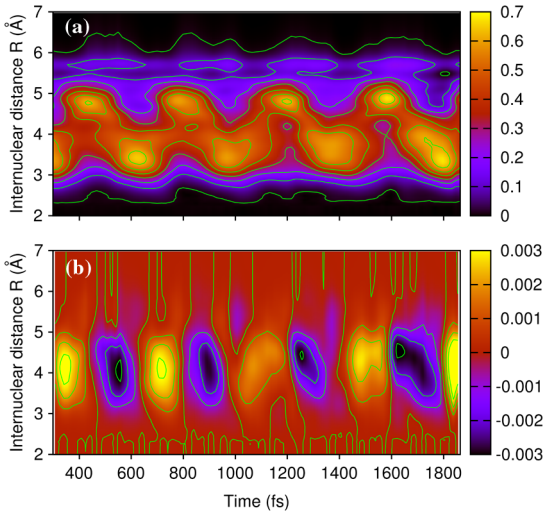

FIG. 1 (color online). (a) Contour plots of the experimental nuclear probability density $\tilde{\rho}(R, t)$ (adapted from Ref. [9]) and (b) the deduced experimental flux density $\tilde{j}_R(R, t)$ for vibrating $Na_2(2^1\Pi_g)$. Equidistant contours are drawn for $\tilde{\rho}(R, t) = 0.01, 0.11, \ldots, 0.61$ Å^{-1} and for $\tilde{j}_R(R, t) = -0.003, -0.002, \ldots, 0.003$ fs^{-1}, respectively.

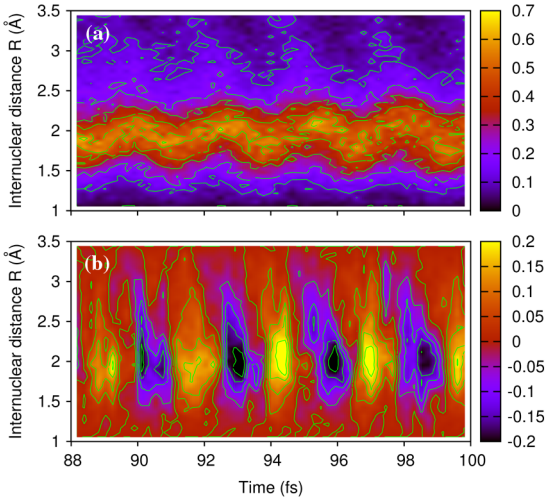

FIG. 2 (color online). (a) Contour plots of the experimental nuclear probability density $\tilde{\rho}(R, t)$ (adapted from Ref. [10]) and (b) the deduced experimental flux density $\tilde{j}_R(R, t)$ for vibrating $D_2^+(^2\Sigma_g^+)$. Equidistant contours are drawn for $\tilde{\rho}(R, t) = 0.01, 0.11, \ldots, 0.61$ Å^{-1} and for $\tilde{j}_R(R, t) = -0.20, -0.15, \ldots, 0.20$ fs^{-1}, respectively.

$Na_2(2^1\Pi_g)$ with rather low intensity of the pump pulse, $\sim 1.0 \times 10^{11}$ W/cm^2 [9].

Once the nuclear probability density $\tilde{\rho}(R, t)$ of a vibrating molecule is measured, it is straightforward to determine the nuclear flux density $\tilde{j}_R(R, t)$. For this purpose, the continuity equation

$$\frac{\partial}{\partial t}\rho + \nabla \cdot \mathbf{j} = 0 \tag{1}$$

is decomposed into radial (R) and angular (Θ, Φ) components ($\mathbf{j} = j_R\mathbf{e}_R + j_\Theta\mathbf{e}_\Theta + j_\Phi\mathbf{e}_\Phi$) and integrated over all orientations. The experimental scenarios—isotropic initial distributions, excitations by linearly z-polarized laser pulses—imply that the angular components do not contribute. Hence Eq. (1) is reduced to the radial part

$$\frac{\partial}{\partial t}\tilde{\rho}(R, t) + \frac{\partial}{\partial R}\tilde{j}_R(R, t) = 0, \tag{2}$$

where $\tilde{j}_R(R, t) = \iint d\Omega \Re[\psi^*(R, \Theta, \Phi, t)(\hat{P}_R/M) \times \psi(R, \Theta, \Phi, t)]$ with radial momentum operator $\hat{P}_R = -i\hbar\partial/\partial R$ and reduced molecular mass M; $\Re$ stands for the real part. The boundary conditions

$$\tilde{j}_R(R, t) \to 0 \quad \text{for} \quad R \to 0 \quad \text{and} \quad R \to \infty \tag{3}$$

then yield

$$\tilde{j}_R(R, t) = -\frac{\partial}{\partial t}\int_0^R dR' \tilde{\rho}(R', t). \tag{4}$$

High resolution of the experimental data for $\tilde{\rho}(R, t)$, as in Refs. [9,10], is essential for accurate numerical evaluations of $\tilde{j}_R(R, t)$ by Eq. (4). Analogous expressions for nuclear fluxes have been derived by W. H. Miller [21–23].

Let us now determine the experimental nuclear flux densities $\tilde{j}_R(R, t)$ for vibrating $Na_2(2^1\Pi_g)$ and $D_2^+(^2\Sigma_g^+)$, using Eq. (4) with the pump-probe spectral results for $\tilde{\rho}(R, t)$ of Refs. [9,10] as inputs. This requires some preparatory steps. First, the original experimental data for $\tilde{\rho}(R, t)$ of $Na_2(2^1\Pi_g)$ contain some background. This is subtracted so that $\tilde{\rho}(R, t) \to 0$ for $R \to 0$ and $R \to \infty$. Second, the experimental data are affected by noise. For compensation, the nuclear densities are renormalized so that $\int_0^\infty dR' \tilde{\rho}(R', t) = 1$ at all times. Third, the lower and upper bounds for normalization, and also for the integral (4), are replaced by values $R_{\min}$ and $R_{\max}$ such that $\tilde{\rho}(R, t)$ is negligible for $R < R_{\min}$ or $R > R_{\max}$.

The resulting experimental nuclear flux densities in vibrating $Na_2(2^1\Pi_g)$ and $D_2^+(^2\Sigma_g^+)$ are shown in Figs. 1(b) and 2(b), respectively. On first glance, they confirm the anticipated classical phenomena: alternating bond stretches and compressions, which are visible in the nuclear densities $\tilde{\rho}(R, t)$, correspond to alternating positive and negative values of the nuclear flux densities $\tilde{j}_R(R, t)$, respectively. The four vibrational periods of the $\tilde{\rho}(R, t)$ illustrated in Figs. 1(a) and 2(a) are thus associated with eight lobes of $\tilde{j}_R(R, t)$ with alternating signs, shown in Figs. 1(b) and 2(b), respectively. Apparently, the formation of lobes of $\tilde{j}_R(R, t)$ with opposite signs is even more prominent than the corresponding oscillatory ridges of the $\tilde{\rho}(R, t)$. By extrapolation, it is easier to analyze the experimental $\tilde{j}_R(R, t)$ than $\tilde{\rho}(R, t)$, in order to discover time-dependent quantum effects. Below, we unravel four new quantum effects (QEs), labeled QE1–QE4.

QE1: The experimental nuclear flux densities for $Na_2(2^1\Pi_g)$ show that the major component of bond compression from ~5.0 to 3.0 Å is followed by a minor component from ~6.0 to 5.0 Å. Likewise for $D_2^+(^2\Sigma_g^+)$, the negative lobes of the experimental nuclear flux densities have two peaks, indicating that bond compression proceeds in two steps, from values of R near 2.5 Å to smaller ones, close to 2.0 Å.

QE2: For $D_2^+(^2\Sigma_g^+)$, not only bond compressions but also bond stretches tend to start at rather large (~ 3 Å) bond distances.

QE3: The small amplitude vibrations of the top of the "mountain" of the nuclear density $\tilde{\rho}(R, t)$ for $D_2^+(^2\Sigma_g^+)$ correspond to much larger amplitudes (~ 0.8 Å) of the $\tilde{j}_R(R, t)$. This means that the apparent shaking of the "mountain" top is due to quasiperiodic large-amplitude "landslides" of a small fraction of the nuclear density—a special quantum effect caused by the very strong field of the pump pulse, which becomes obvious in phase (ii) of molecular vibrations.

QE4: Another quantum effect can be seen in snapshots of the nuclear flux densities during molecular vibrations. Figure 3 shows the experimental $\tilde{j}_R(R, t)$ [and for comparison also $\tilde{\rho}(R, t)$] of the vibrating $Na_2(2^1\Pi_g)$, in the time window from 358 to 558 fs when the molecular stretch turns to compression. The switch occurs close to $t =$ 458.1 fs. The corresponding classical expression $j_{\rm cl}(R, t) = \rho_{\rm cl}(R, t)v_{\rm cl}$ would suggest that this turn should be associated with a moment when the classical density $\tilde{\rho}_{\rm cl}(R, t)$ is localized at the classical turning point and the velocity $v_{\rm cl}$ is equal to zero; i.e., $j_{\rm cl}(R, t)$ should vanish. In contrast, at $t = 458.1$ fs, the experimental $\tilde{j}_R(R, t)$ approaches rather small absolute values (compared to the maximum ones), but it never vanishes. Instead, it is dispersed over rather large domains of bond lengths, from $R \sim 3$ to 6.0 Å, with two changes of sign at $R = 3.7$ Å and $R = 5.3$ Å, corresponding to bond stretches at small and large values of R but bond compression at medium bond lengths. Vibrational reversals of $\tilde{j}_R(R, t)$ are predicted in Refs. [7,24,25] as a consequence of wave packet interference—here this is revealed by high resolution pump-probe spectroscopy. The cartoon in the very bottom of Fig. 3 illustrates this phenomenon as the "quantum accordion." In the (idealized, one-dimensional) classical accordion, there is a moment in which all the bellows remain still as push turns to pull. In contrast, the bellows in the "quantum accordion" never stand still altogether, but during the turn from pull to push, different parts expand

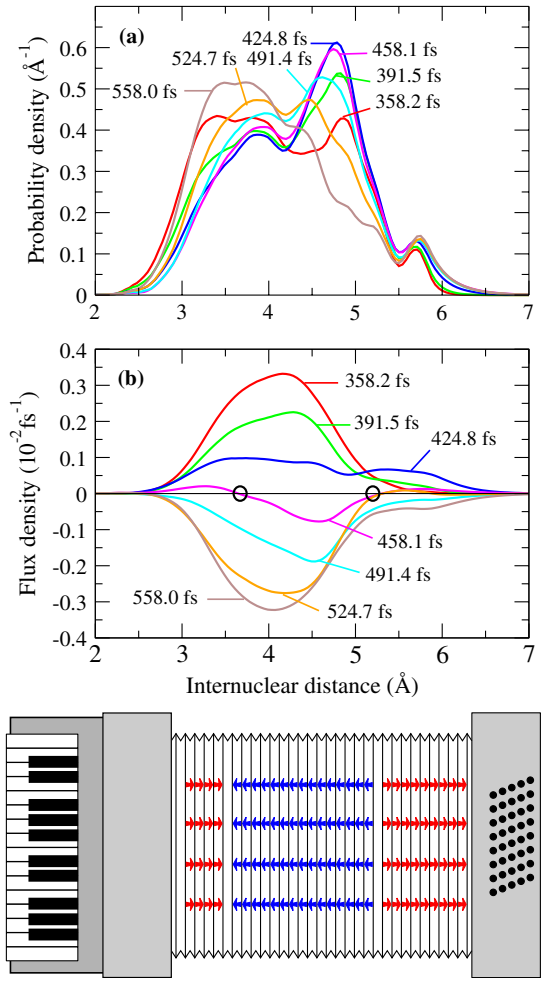

FIG. 3 (color online). (a) Snapshots of the experimental nuclear probability density $\tilde{\rho}(R, t)$ (adapted from Ref. [9]) and (b) the deduced experimental flux density $\tilde{j}_R(R, t)$ for vibrating $Na_2(2^1\Pi_g)$. Bottom panel illustrates the "quantum accordion," which corresponds to the snapshot of $\tilde{j}_R(R, t)$ at $t = 458.1$ fs, with two changes of the directions of the nuclear flux density marked by circles (see text).

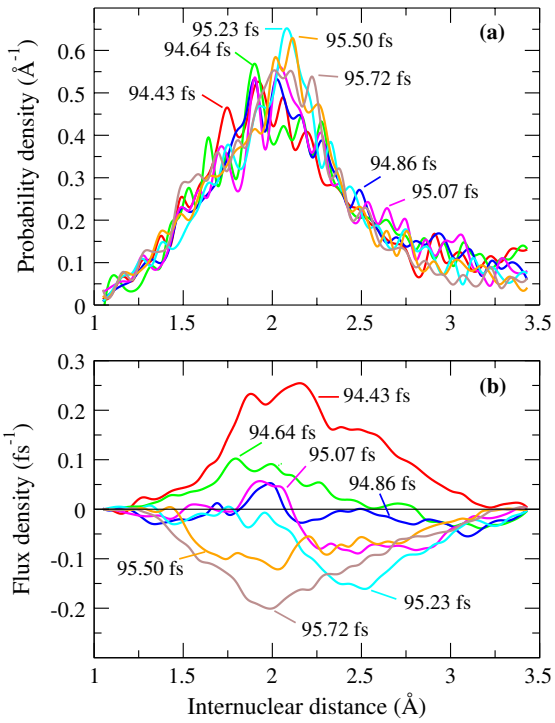

FIG. 4 (color online). (a) Snapshots of the experimental nuclear probability density $\tilde{\rho}(R, t)$ (adapted from Ref. [10]) and (b) the deduced experimental flux density $\tilde{j}_R(R, t)$ for vibrating $D_2^+(^2\Sigma_g^+)$.

or contract in opposite directions. Figure 4 shows similar snapshots for vibrating $D_2^+(^2\Sigma_g^+)$. Apparently, the "quantum accordion" is even more pronounced for the light D_2^+ compared to the heavy Na_2. For example, $\tilde{j}_R(R, t)$ for D_2^+ at $t = 95.07$ fs exhibits not just two but four changes of sign. Comparison with the previous and next snapshots at 94.86 and 95.23 fs show that between formation and annihilation, the nodes of $\tilde{j}_R(R, t)$ move by distances of the order of 10 pm within 200 asec.

Quantitatively, the quantum effects QE1–QE4 depend on the quality of the densities $\tilde{\rho}(R, t)$, which in turn depend on the quality of the underlying pump-probe spectra and the method of extracting $\tilde{\rho}(R, t)$ [9,10]. Qualitatively, however, the effects are robust with respect to small experimental uncertainties $\Delta\tilde{\rho}(R, t)$. The corresponding uncertainty in $\tilde{j}(R, t)$ is $\Delta\tilde{j}(R, t) = -(\partial/\partial t)\int_0^R dR'\Delta\tilde{\rho}(R', t)$. The normalization of the density implies $\int_0^\infty \Delta\tilde{\rho}(R, t)dR = 0$. In general, $\Delta\tilde{\rho}$ would have a random distribution of signs; hence, the mean relative deviations of the flux density $\langle|\Delta\tilde{j}/\tilde{j}|\rangle$ are much smaller than those of the density $\langle|\Delta\tilde{\rho}/\tilde{\rho}|\rangle$ due to the cancellation along the integration range. In conclusion, the flux densities are robust with respect to small changes of the densities.

In summary, this Letter presents the first experimentally determined nuclear flux densities in molecules, revealing fascinating quantum effects. These are important for several fields of physics, including attosecond and strong field physics [26–28], and neighboring fields such as femtosecond chemistry [18]. Unraveling these effects by the present approach profits from the fact that flux densities are much more sensitive to time-dependent quantum effects than probability densities. A similar conjecture has been made in the recent quantum dynamical investigations of symmetry breaking in tunneling in cyclic versus noncyclic double wells: the densities are practically indistinguishable, whereas the flux densities are entirely different [29].

The present approach may be applied to high resolution pump-probe results for densities $\tilde{\rho}(R, t)$ of arbitrary homonuclear diatomic molecules or ions. The results for $D_2^+(^2\Sigma_g^+)$ provide the highest spatiotemporal resolution (5 pm, 220 asec) of any flux density that has ever been measured in physics. This is the first step into this uncharted territory. It should stimulate high-resolution pump-probe

measurements of vibrating diatomic molecules, beyond the present systems $Na_2(2^1\Pi_g)$ [9] and $D_2^+(^2\Sigma_g^+)$ [10] (see also Refs. [30,31]). The present approach can also be applied to competing processes in diatomic molecules or molecular ions, such as dissociations and electronically nonadiabatic transitions. Extensions to nonspherically integrated signals (these have also been documented in Ref. [10]) or to polyatomic molecules are more demanding, in that they require use of the three-dimensional version of the continuity equation (1) with modified boundary conditions (3). Recent concepts for monitoring molecular motions by means of high-harmonic generation [32] and x-ray phase contrast imaging [33] hold promise for direct access to intramolecular fluxes.

We would like to express our gratitude to Professor T. Baumert (Kassel), Professor J. Ullrich (Heidelberg and Braunschweig), and Dr. R. Moshammer (Heidelberg) for providing the experimental data for the nuclear densities of the vibrating $Na_2(2^1\Pi_g)$ and $D_2^+(^2\Sigma_g^+)$ as published in Refs. [9,10], respectively. We also thank them, as well as Professor D. J. Diestler (Lincoln) and Professor V. Engel (Würzburg) for valuable advice, and Mr. F. Korinth for drawing the quantum accordion in Fig. 3. Support of our cooperation by Professor S. Jia, Professor L. Xiao (Taiyuan), and Professor B. Paulus (Berlin) has been inciting. This work profits from financial support, in part from Deutsche Forschungsgemeinschaft under Grant No. Ma 515/25-1, 973 Program of China under Grant No. 2012CB921603, the National Natural Science Foundation of China under Grant No. 11004125, and Major Program of the National Natural Science Foundation of China under Grant No. 10934004.

*jmanz@chemie.fu-berlin.de

[1] Heraclitus, Fragment 49aDK (~−492) .
[2] D. R. Herschbach, Angew. Chem., Int. Ed. Engl. **26**, 1221 (1987) (Nobel Lecture) .
[3] Y. T. Lee, Angew. Chem., Int. Ed. Engl. **26**, 939 (1987) (Nobel Lecture).
[4] A. Nitzan and M. A. Ratner, Science **300**, 1384 (2003).
[5] *Current-Driven Phenomena in Nanoelectronics*, edited by T. Seideman (Pan Stanford Publishing, Singapore, 2010).
[6] A. N. Pfeiffer, C. Cirelly, M. Smolarski, D. Dimitrovski, M. Abu-samha, L. B. Madsen, and U. Keller, Nat. Phys. **8**, 76 (2012).
[7] T. Bredtmann, H. Katsuki, J. Manz, K. Ohmori, and C. Stemmle, Mol. Phys. **111**, 1691 (2013).
[8] E. Schrödinger, Ann. Phys. (Leipzig) **81**, 109 (1926).
[9] T. Frohnmeyer and T. Baumert, Appl. Phys. B **71**, 259 (2000).
[10] T. Ergler, A. Rudenko, B. Feuerstein, K. Zrost, C. D. Schröter, R. Moshammer, and J. Ullrich, Phys. Rev. Lett. **97**, 193001 (2006).
[11] C. Meier and V. Engel, Chem. Phys. Lett. **212**, 691 (1993).
[12] B. Feuerstein and U. Thumm, Phys. Rev. A **67**, 063408 (2003).
[13] A. Assion, M. Geisler, J. Helbing, V. Seyfried, and T. Baumert, Phys. Rev. A **54**, R4605 (1996).
[14] M. Seel and W. Domcke, J. Chem. Phys. **95**, 7806 (1991).
[15] S. Chelkowski, P. B. Corkum, and A. D. Bandrauk, Phys. Rev. Lett. **82**, 3416 (1999).
[16] E. R. Hosler and S. R. Leone, Phys. Rev. A **88**, 023420 (2013).
[17] A. H. Zewail, Science **242**, 1645 (1988).
[18] A. H. Zewail, Angew. Chem., Int. Ed. **39**, 2586 (2000) (Nobel Lecture).
[19] I. S. Averbukh, M. J. J. Vrakking, D. M. Villeneuve, and A. Stolow, Phys. Rev. Lett. **77**, 3518 (1996).
[20] A. D. Bandrauk, E. Aubanel, and S. Chelkowski, in *Femtosecond Chemistry*, edited by J. Manz and L. Wöste (VCH Verlagsgesellschaft, Weinheim, 1995), p. 731.
[21] W. H. Miller, J. Chem. Phys. **61**, 1823 (1974).
[22] W. H. Miller, Acc. Chem. Res. **26**, 174 (1993).
[23] U. Manthe, T. Seideman, and W. H. Miller, J. Chem. Phys. **101**, 4759 (1994).
[24] D. J. Diestler, A. Kenfack, J. Manz, and B. Paulus, J. Phys. Chem. A **116**, 2736 (2012).
[25] D. J. Diestler, A. Kenfack, J. Manz, B. Paulus, J. F. Pérez-Torres, and V. Pohl, J. Phys. Chem. A **117**, 8519 (2013).
[26] F. Krausz and M. Ivanov, Rev. Mod. Phys. **81**, 163 (2009).
[27] H. Niikura, H. J. Wörner, D. M. Villeneuve, and P. B. Corkum, Phys. Rev. Lett. **107**, 093004 (2011).
[28] J. B. Bertrand, H. J. Wörner, P. Salières, D. M. Villeneuve, and P. B. Corkum, Nat. Phys. **9**, 174 (2013).
[29] T. Grohmann, J. Manz, and A. Schild, Mol. Phys. **111**, 2251 (2013).
[30] D. Ray, F. He, S. De, W. Cao, H. Mashiko, P. Ranitovic, K. P. Singh, I. Znakovskaya, U. Thumm, G. G. Paulus, M. F. Kling, I. V. Litvinyuk, and C. L. Cocke, Phys. Rev. Lett. **103**, 223201 (2009).
[31] Y. H. Jiang *et al.*, Phys. Rev. A **81**, 051402 (2010).
[32] S. Chelkowski, T. Bredtmann, and A. D. Bandrauk, Phys. Rev. A **85**, 033404 (2012).
[33] G. Dixit, J. M. Slowik, and R. Santra, Phys. Rev. Lett. **110**, 137403 (2013).